Insect Biochemistry and Molecular Biology 114 (2019) 103225

Contents lists available at ScienceDirect

Insect Biochemistry and Molecular Biology

journal homepage: www.elsevier.com/locate/ibmb

A tandem death effector domain-containing protein inhibits the IMD signaling pathway via forming amyloid-like aggregates with the caspase-8 homolog DREDD

Jie Hu[a], Xinyi Wang[a], Xiaoyi Xiao[a], Chang Sun[a], Qingyou Xia[a,b], Fei Wang[a,b,*]

[a] Biological Science Research Center, Southwest University, Chongqing, China
[b] Chongqing Key Laboratory of Sericultural Science, Chongqing Engineering and Technology Research Center for Novel Silk Materials, Southwest University, Chongqing, China

ARTICLE INFO

Keywords:
Caspase-8 like
DREDD
IMD pathway
Death effector domain
Amyloidal aggregates

ABSTRACT

Negative regulation of the immune signaling pathway involves diverse negative regulators that target different signaling molecules. One of the signaling molecules, DREDD, which activates the NF-κB transcription factor Relish in the IMD pathway, is a homolog of mammalian caspase-8. Some structural related proteins have been identified to regulate the activity of caspase-8 in signaling complex assembly. However, it is unknown in insects whether the IMD pathway undergoes such a down-regulation. In this study, we explored the regulatory role of a newly identified protein BmCaspase-8 like (BmCasp8L) in silkworm, which displays high sequence similarity with the N-terminus of BmDREDD to the IMD pathway, and investigated its mechanism. Domain prediction, phylogenic analysis and gene architecture suggests BmCasp8L acts as a potential inhibitor to BmDREDD. We then found it is highly expressed in the fat body and hemocytes, and suppresses the cleavage of BmRelish and BmIMD mediated by BmDREDD upon PGN stimulation, resulting in deficiency in antimicrobial peptides production. Besides the inhibitory role in the IMD pathway, it also suppresses the BmDREDD-induced apoptosis. By investigating the amyloidal activity of BmCasp8L and its interaction with BmDREDD and BmFADD, we demonstrated that BmCasp8L forms amyloid-like aggregates *in vitro* as well as *in vivo*, and it inactivates BmDREDD by blending into the amyloidal speck-like structure formed by BmDREDD and BmFADD that is required for BmDREDD activity. Taken together, our results demonstrate BmCasp8L inhibits the IMD signaling pathway via forming amyloidal aggregates with BmDREDD, suggesting an evolutionarily conserved regulatory mechanism of innate immune signaling pathway.

1. Introduction

As one of the two major NF-κB signaling pathways that mediate innate immune response in insects, the immune deficiency (IMD) pathway has been so intensively studied that how extracellular signals are relayed from germ line-encoded receptors to downstream NF-κB transcription factor is generally outlined (Kleino and Silverman, 2014; Myllymaki et al., 2014). Once the NF-κB transcription factor Relish which is normally restrained in the cytoplasm is activated, it translocates into the nucleus and induces the production of a plethora of effector molecules, including antimicrobial peptides (AMPs). Besides its critical role in defending Gram-negative bacterial infection, IMD pathways is also implicated in regulating homeostasis, since commensal dysbiosis, tissue damage or short lifespan, has been reported as the result of hyper-activation or des-regulation of the signaling pathway (Bonnay et al., 2013; Dantoft et al., 2013, 2016; Kounatidis et al., 2017; Libert et al., 2006). Therefore, exploring the negative regulatory mechanism is necessary for understanding the coordination of immune response with other physiological processes.

The IMD pathway is activated when membrane-bound peptidoglycan recognition protein (PGRP)-LC or intracellular PGRP-LE recognizes diaminopimelic acid-type peptidoglycan (DAP-PGN) derived from Gram-negative bacteria and certain Gram-positive bacteria, such as *Bacillus* spp., then the signal is delivered sequentially through IMD, Fas associated via death domain (FADD) and caspase-8 homolog Death related ced-3/Nedd2-like caspase (DREDD), which subsequently cleaves IMD and Relish (Akira et al., 2006; Kim et al., 2014; Royet et al., 2005). Cleavage of IMD allows its polyubiquination and recruitment of transforming growth factor (TGF)-activated kinase 1 (TAK1), which in turn activates IκB kinase (IKK) complex, and eventually leads to Relish

* Corresponding author. Biological Science Research Center, Southwest University, Chongqing, China.
E-mail addresses: fwangswu@gmail.com, massmoca@swu.edu.cn (F. Wang).

https://doi.org/10.1016/j.ibmb.2019.103225
Received 28 May 2019; Received in revised form 8 August 2019; Accepted 21 August 2019
Available online 22 August 2019
0965-1748/

phosphorylation (Erturk-Hasdemir et al., 2009; Kleino et al., 2005; Paquette et al., 2010). Cleavage of Relish, on the other hand, releases it from the sequestering ankyrine-repeat domain on its own C-terminal tail, resulting in nucleus transportation (Stöven et al., 2000, 2003). Mutant or RNAi screening in *Drosophila* helped to identify diverse negative regulators which may target the same signaling molecule but with distinct mechanism (Foley and O'Farrell, 2004; Kim et al., 2006; Maillet et al., 2008; Morris et al., 2016). A majority of them inactivate or promote the degradation of signaling molecules by modifying their ubiquitination status (Engel et al., 2014), a few others may execute inhibitory role by disrupting the interaction between signaling molecules, which relies on mutual availability of certain structures on each other. For instance, Poor IMD response upon knock-in (Pirk) interferes with the amyloid-like fibrils formed by PGRP-LC, PGRP-LE and IMD through their cryptic RIP homotypic interaction motifs (cRHIMs) (Kleino et al., 2017; Kleino and Silverman, 2019). Since activation of Relish is a decisive step in the IMD pathway, both of Relish phosphorylation and cleavage requires DREDD, making it an important target subject to negative regulation.

Interestingly, the IMD pathway has been considered to be evocative of the mammalian TNF-α receptor signaling pathway, since their signaling molecules share striking similarity (Georgel et al., 2001). Parallels between receptor-interacting protein kinase (RIP) and IMD, mammalian FADD and insect FADD, caspase-8 and DREDD suggest these two pathways may share the same regulatory mechanism. Upon TNF receptor activation by the ligands, FADD recruits caspase-8 at the death-inducing signaling complex (DISC) through their death effector domains (DEDs), leading to the formation of caspase-8 filaments (Riley et al., 2015; Siegel et al., 1998). Moreover, this assembly is the target for some tandem DED-containing proteins, such as cellular FLICE (FADD-like IL-1β-converting enzyme)/Casp-8-like-inhibitory protein (cFLIP) (Horn et al., 2017; Schleich et al., 2016), which made us wonder whether DREDD and FADD in insects form such a cytoplasmic structure, and any molecule may inhibit the IMD pathway by interacting with them.

Recently, we discovered a novel protein with high sequence similarity to the N-terminus of BmDREDD in silkworm, *Bombyx mori* and named it BmCaspase-8-like (BmCasp8L) (Hua et al., 2018). It inhibited the cleavage of BmRelish and production of *BmCecropinA1* under DAP-PGN stimulation, suggesting it may act as a negative regulator of the IMD pathway (Hu et al., 2018). In the present study, we found BmCasp8L not only suppresses the BmDREDD-mediated cleavage of both BmIMD and BmRelish, but its pro-apoptotic activity. Further, we found BmCasp8L displays amyloidal activity as evidenced by amyloid dye binding assays and semi-denaturing detergent agarose gel electrophoresis (SDD-AGE), and via interaction with both BmFADD and BmDREDD, it is comingled into the aggregates formed by these two signaling molecules. Collectively, our results demonstrate that BmCasp8L acts as a regulator of signaling amyloid formation in the IMD pathway, suggesting an evolutionary conservation in regulatory mechanism of innate immune signaling.

2. Materials and methods

2.1. Cells, insects and antibodies

BmE cells were maintained at 27 °C in Grace medium (Gibco, Carlsbad, CA, USA) supplemented with 10% FBS and penicillin and streptomycin (Hyclone, Logan, UT, USA). Silkworm DaZao P50 strain was originally obtained from Silkworm Genetic Resource Supply in Southwest University. Larvae were reared with fresh mulberry leaves at 27 °C under 12 h light/12 h dark cycles. The following antibodies have been used: anti-FLAG mouse monoclonal Ab (Sigma-Aldrich, St Louis, MO, USA), anti-Myc mouse monoclonal Ab (Invitrogen, Carlsbad, CA, USA), anti-HA mouse monoclonal Ab (Invitrogen), anti-Tubulin mouse monoclonal Ab (Beyotime, Shanghai, China) and anti-V5 mouse monoclonal Ab (Abcam, Cambridge, UK). Rabbit polyclonal antibody against BmCasp8L was generated by Novoprotein (Shanghai, China).

2.2. Plasmid construction, dsRNA synthesis and cell transfection

Bmfadd and *BmIMD* was cloned from silkworm larvae cDNA. Expression plasmids containing N-terminal FLAG tagged-BmCasp8L (FLAG-BmCasp8L), HA tagged-BmFADD (HA-BmFADD), C-terminal Myc tagged-BmIMD (BmIMD-Myc) and N-terminal V5 tagged-BmDREDD (V5-BmDREDD) was constructed following the same procedures of construction of Myc tagged-BmRelish (Myc-BmRelish) (Hua et al., 2016). Fluorescent protein tagged constructs, including BmDREDD-mCherry, BmFADD-EGFP, BmCasp8L-EGFP and BmCasp8L-YFP were also constructed by the same methods.

Interfering dsRNA against *Bmcasp8L* (dsCasp8L) or *egfp* (dsEGFP) was generated using T7 *in vitro* Transcription Kit (Promega, Fitchburg, WI, USA) following the manufacturer's instruction. Primers used in this study were listed in Supplementary Table 1.

Cells were seeded in an appropriate cell culture plate and incubated overnight. Plasmids or dsRNA were transiently transfected into cells using X-treme GENE transfection reagent (Roche, Basel, Switzerland) following the manufacturer's instruction.

2.3. Infection experiments

Silkworm larvae were injected with dsRNA (20 μg/larvae) through the second last stoma in abdomen with a fine needle at second day of fifth instar. 24 h later, overnight-cultured *Serratia marcescens* (1×10^3/larvae) or ddH_2O were injected at the same site. Silkworm larvae were collected and anti-microbial peptides were examined at different time points for qRT-PCR.

2.4. Quantitative RT-PCR (qRT-PCR) analysis

Total RNA was extracted from whole silkworm larvae or BmE cells using Total RNA kit (Omega, Atlanta, GA, USA) and reverse transcribed by 5 × PrimeScript RT Master Mix (Takara, Japan). qRT-PCR was performed using SYBR Premix Ex Taq II (Takara). The expression level of *Bmcasp81*, *BmCecropinA1*, *BmCecropinB* and *BmAttacin* was normalized to the control (SilkDB probe number: sw22934). Primers used in qRT-PCR were listed in Supplementary Table 1.

2.5. Luciferase reporter assay

BmE cells were transfected with 1 μg BmCasp8L-expressing constructs together with 0.5 μg Firefly luciferase reporter and 0.05 μg Renilla luciferase plasmid. 24 h after transfection, cells were treated with 10 μg/ml DAP-PGN (Sigma) for 12 h. Luciferase activity was measured using Dual-Glo luciferase Reporter Assay System (Promega) following the manufacturer's instruction. Firefly luciferase readings were divided by the Renilla luciferase readings to calculate the relative fold change.

2.6. Immunoprecipitation and immunoblotting

Cells were lysed in NP40 lysis buffer (Beyotime) and the concentration was determined by BCA assay. 5 μg antibodies as indicated in figures was incubated with 25 μL Protein A/G Agarose (Beyotime) followed by incubation with 500 μg total protein for 6 h at 4 °C. The immunoprecipitates were washed for 5 times and subjected to immunoblotting. For immunoblotting analysis, whole cell lysates or immunoprecipitates were separated by SDS-PAGE and transferred to PVDF membrane. The membrane was incubated with respective antibodies and the protein bands were visualized using Super Signal West Femto detection system (Thermo Scientific, Waltham, MA, USA).

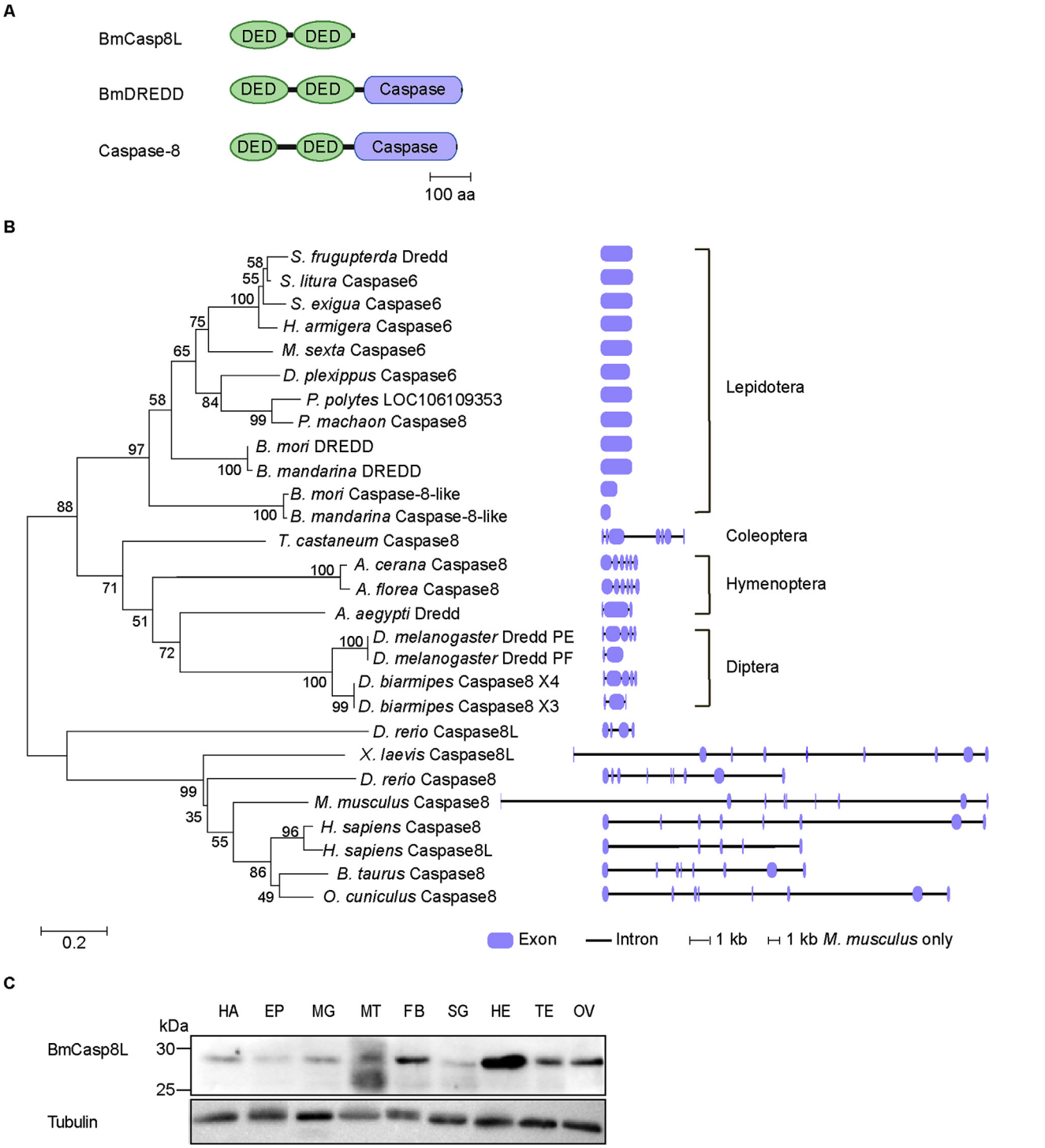

Fig. 1. Domain structure, phylogenic analysis and tissue-specific expression of BmCasp8L. (A) Schematic representation of the domain structure of BmCasp8L, BmDREDD and capase-8. (B) Molecular phylogenic tree and gene architecture of caspase-8 homologs from various species. The tree was generated using the neighbor-joining method. Numbers on nodes indicate bootstrap values from 1000 replications. (C) Tissue-specific expression of BmCasp8L in silkworm larvae on 3 day of 5th instar. HA, head; EP, epidermis; MG, midgut; MT, Malphghian tubule; FB, fat body; SG, silk gland; HE, hemocyte; TE, testis; OV, ovary.

2.7. Confocal microscopy

BmE cells grown on coverslips in 12-well plate were transfected with Casp8L-YFP, Casp8L-EGFP, DREDD-mCherry or FADD-EGFP-expressing constructs alone or in combination in the presence of 50 mM zVAD-FMK. Cells were fixed with 4% PFA for 20 min. Then they were gently rinsed with PBS and permeabilized with 0.3% Triton X-100, followed by staining with 3 mM Thioflavin T (Santa Cruz Biotechnologies, Dallas, TX, USA) in ethanol:PBS (30:70) for 20 min. Next, cells were washed 3 times in 70% ethanol and 5 times in PBS. Finally, cells were stained with DAPI (Beyotime) for 10 min and imaged under a ZEISS LSM 880 confocal microscope with a 63 × oil immersion objective using sequential scanning. ThT was excited at 458 nm and emission detected at 485–530 nm, mCherry was excited at 587 nm and emission detected at 610 nm, EGFP was excited at 488 nm and emission detected at 509 nm, YFP was excited at 513 nm and emission detected

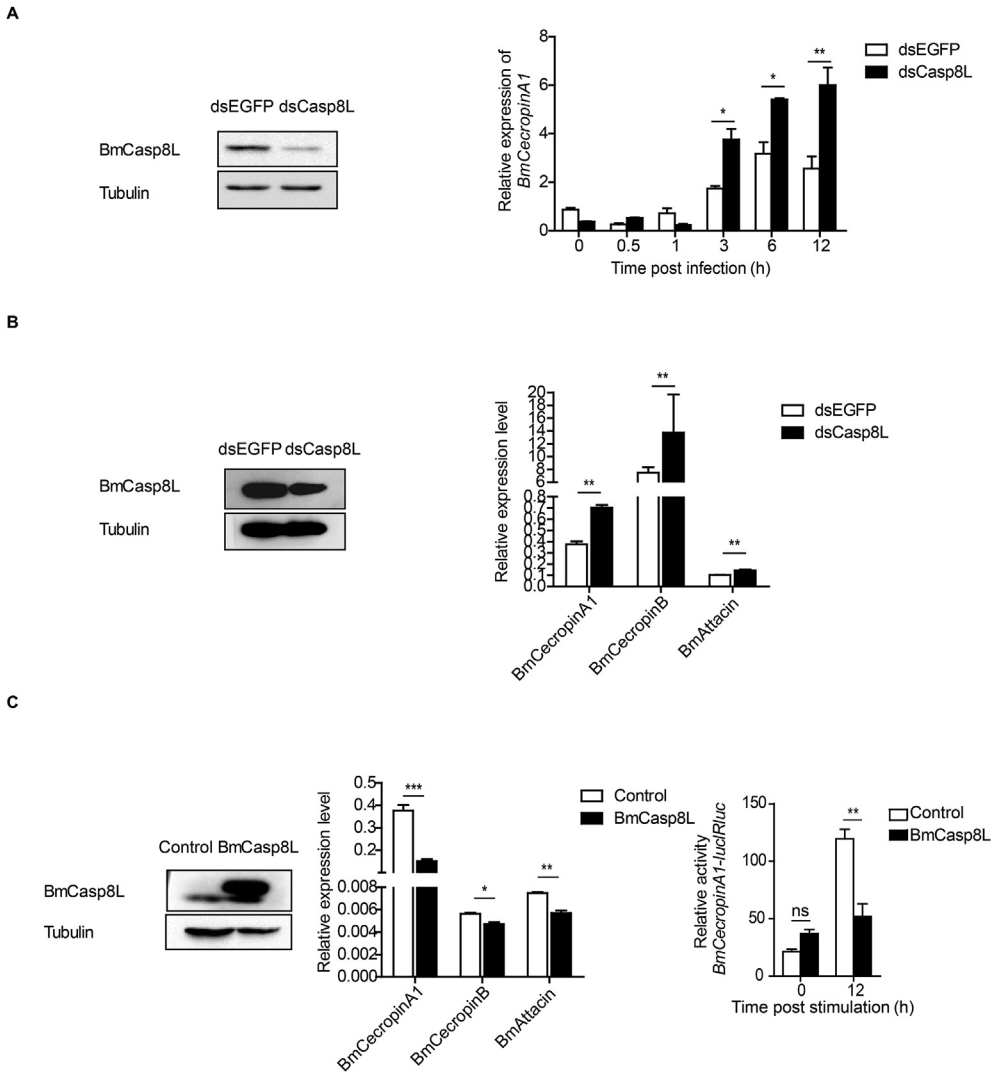

Fig. 2. BmCasp8L negatively regulates immune response by suppressing the expression of antimicrobial peptides. (A) qRT-PCR analysis assessing the mRNA level of *BmCecropinA1* after BmCasp8L was knocked down by dsRNA in silkworm larvae at different time points post *S. marcescens* infection. (B) qRT-PCR analysis assessing the mRNA level of *BmCecropinA1*, *BmAttacin* and *BmCecropinB* when BmCasp8L was knocked down by dsRNA in BmE cells at 12 h post DAP-PGN stimulation. (C) qRT-PCR analysis assessing the mRNA level of *BmCecropinA1*, *BmAttacin* and *BmCecropinB* and luciferase assay of *BmCecropinA1*-luciferase reporter at 12 h post DAP-PGN stimulation when BmCasp8L was over-expressed in BmE cells. The results of qRT-PCR analysis and lucifierase assay are given as the mean ± S.D. (n = 3). Statistical significance was assessed using Student's *t*-test. $*p < 0.05$, $**p < 0.01$, $***p < 0.001$.

at 527 nm, DAPI was excited at 358 nm and emission detected at 461 nm.

2.8. Transmission electron microscopy (TEM)

The ultrastructure of protein aggregates was observed under transmission electron microscope. The purified BmCasp8L protein was loaded on carbon-coated cooper TEM grids. After incubation for 1 min and air dried, the samples were negatively stained with 2% uranyl acetate for 45 s. Then excess stain was removed and the samples were left to dry. Images were obtained using Talos F200X transmission electron microscope (Czech Republic) operating at 200 kV.

2.9. Semi-denaturing detergent agarose gel electrophoresis (SDD-AGE)

To analyze detergent resistant protein aggregates in cell, lysates of BmE cells transfected with FLAG-BmCasp8L, HA-BmFADD, V5-BmDREDD, were mixed with 4 × protein loading buffer (2 × TBE, 20% Glycerol, 8% SDS, 0.2% Bromophenol blue) at room temperature for 10 min. Samples were separated by electrophoresis in the running buffer (1 × TBE and 0.1% SDS) in a vertical 1.5% agarose gel containing 0.1% SDS for 9 h with a constant voltage of 48 V at 4 °C. Proteins were then transferred to PVDF by capillary transfer, and immunoblotted with corresponding antibodies.

2.10. Apoptotic assay

BmE cells grown in 48-well plate were transfected with FLAG-BmCasp8L or V5-BmDREDD-expressing constructs. 72 h after transfection, cells were washed with PBS, and fixed with 4% PFA for 20 min. Cells were then permeabilized with 0.3% Triton X-100 followed by TUNEL staining (Beyotime). Cells were examined by fluorescence microscopy and apoptotic cells were quantitated by the mean percentage of the FITC fluorescence signs of apoptosis as fraction of the total number of cells counted, about 5 visual fields per sample, at least 80 cells per visual fields.

2.11. Thioflavin T (ThT) fluorimetry

BmCasp8L with N terminal 6 × His-tag were expressed in *E. coli* and purified by affinity chromatography (Novoprotein). 32 μM BmCasp8L, Aβ (Sigma) and BSA was incubated at 37 °C for 24 h in sodium phosphate buffer (pH 7.4) respectively, ThT was added to each test sample to a final concentration of 25 μM. Fluorescence was monitored at excitation of 450 nm and emission of 485 nm.

2.12. Statistics

All data were expressed as means ± SD. Statistical differences between control and treated groups were evaluated using Student's *t-test*

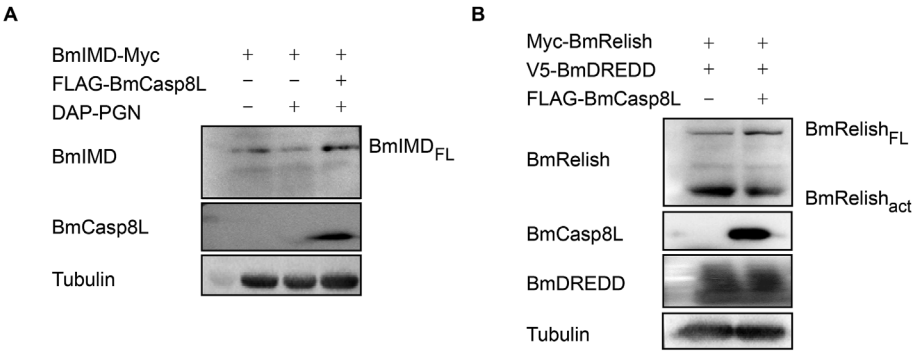

Fig. 3. BmCasp8L inhibits the cleavage of BmRelish and BmIMD mediated by BmDREDD. (A) BmE cells were transfected with BmIMD-Myc alone or together with FLAG-BmCasp8L, then treated with DAP-PGN for 12 h before lysis. Cell lysates were subjected to immunoblotting with anti-Myc, anti-FLAG and anti-Tubulin antibodies. (B–C) Lysates from BmE cells co-transfected with Myc-BmRelish and V5-BmDREDD together with or without FLAG-BmCasp8L (B), or from cells co-transfected with BmIMD-Myc and V5-BmDREDD together with or without FLAG-BmCasp8L (C) were subjected to immunoblotting with anti-Myc, anti-FLAG, anti-V5 and anti-Tubulin antibodies.

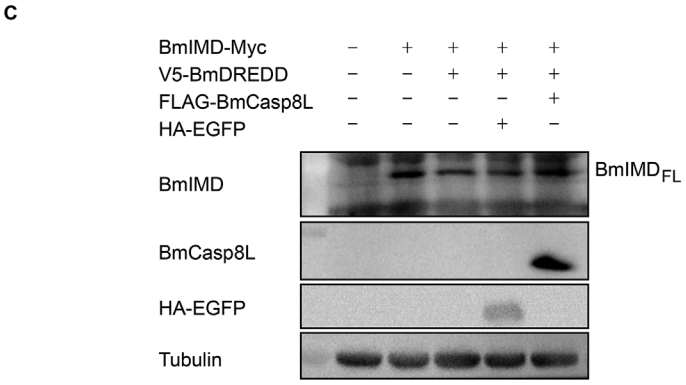

($^{*}p < 0.05$, $^{**}p < 0.01$, $^{***}p < 0.001$).

3. Results

3.1. BmCasp8L is a caspase domain-missing homolog of Caspase-8

Domain analysis predicted tandem DEDs in BmCasp8L, which are similar to the N terminus of BmDREDD and Caspase-8. However, BmCasp8L does not have the C-terminal caspase domain shared by its homologs (Fig. 1A). Due to the lack of comprehensive genomic data in many other insects, Casp8L were only identified in domestic and wild silkworm (Fig. 1B). Interestingly, a truncated isoform of *Drosophila* DREDD, DREDD-PF also lacks the catalytic domain possessed by the full-length isoform DREDD-PE that is usually shortened as DREDD (Di Fruscio et al., 2003). An extensive survey of the gene architecture of *dredd/caspase-8* in various species revealed that it is encoded by multi-exons, except in Lepidoptera, which is encoded by single exon. Alternative splicing of multi-exon gene would generate long and short isoforms, the latter was also reported in human caspase-8, known as caspase-8L that carries a stop codon after the two N-terminal DED repeats and acts as an inhibitor of the caspase-mediated apoptosis (Miller et al., 2006). *Dredd* in Lepidoptera, on the contrary, only encodes the full length protein containing catalytic domain, thus it would be understandable that other protein, such as Casp8L may be the substitute if the counteraction carried out by the caspase domain-missing isoform is vital for normal physiology. Expression of *Bmcasp8l* was detected in all larval tissues, with the highest level in hemocytes and fat bodies (Fig. 1C). Because most antibacterial proteins are expressed predominantly in these organs, the abundance of BmCasp8L implies that BmCasp8L is involved in the immune responses of silkworm.

3.2. BmCasp8L down-regulates the IMD pathway through suppressing the activity of BmDREDD

To explore the function of BmCasp8L in immune response, we synthesized dsRNA (dsCasp8L) to knock down *Bmcasp8l* in larvae and then infected them with *S. marcescens*. A significant increase in *BmCecropinA1* transcript level was observed 3 h after infection compared to dsEGFP-treated controls, and became more prominent at 12 h after infection (Fig. 2A). Similarly, knock-down of *Bmcasp8l* in cells enhanced several AMPs expression, including *BmCecropinA1*, *BmAttacin* and *BmCecropinB* upon PGN stimulation (Fig. 2B). On the contrary, PGN stimulation failed to activate *BmCecropinA1*-luciferase reporter when BmCasp8L was over-expressed, and AMP levels were much lower in those cells compared to control, further suggesting that the activity of the NF-κB transcription factor BmRelish in the IMD pathway was down-regulated (Fig. 2C).

Previously we have identified the cleavage of BmRelish under PGN stimulation is suppressed by BmCasp8L (Hu et al., 2018). Since processing of IMD is also triggered by PGN stimulation, we then examined whether cleavage of BmIMD was affected by BmCasp8L. We co-expressed BmIMD and BmCasp8L in cells and examined the appearance of cleaved form of BmIMD under the stimulation of PGN. Although we was unable to detect the cleaved band in all samples, we found stronger full length (BmIMD$_{FL}$) band was present when BmCasp8L was co-expressed (Fig. 3A), suggesting that less BmIMD$_{FL}$ underwent processing. Considering DREDD is responsible for the cleavage of both Relish and IMD, we suspected BmCasp8L suppresses the activity of BmDREDD. To test it, we introduced BmDREDD into cells instead of PGN stimulation. More BmRelish and BmIMD were present as full length protein (Fig. 3B–C), and less cleaved form of BmRelish (BmRelish$_{act}$) was also observed, consistent with results obtained under PGN stimulation. Taken together, these results suggest BmCasp8L down-regulates the IMD pathway through inactivating BmDREDD.

3.3. BmCasp8L protects cells from BmDREDD-induced apoptosis

Besides cleaving Relish and IMD in response to immune stimulation, DREDD also acts as an initiator caspase and induces apoptosis when over-expressed (Chen et al., 1998; Wang et al., 2016). In order to investigate whether BmCasp8L suppresses the pro-apoptotic function of BmDREDD, apoptotic cells were stained with TUNEL and quantitated.

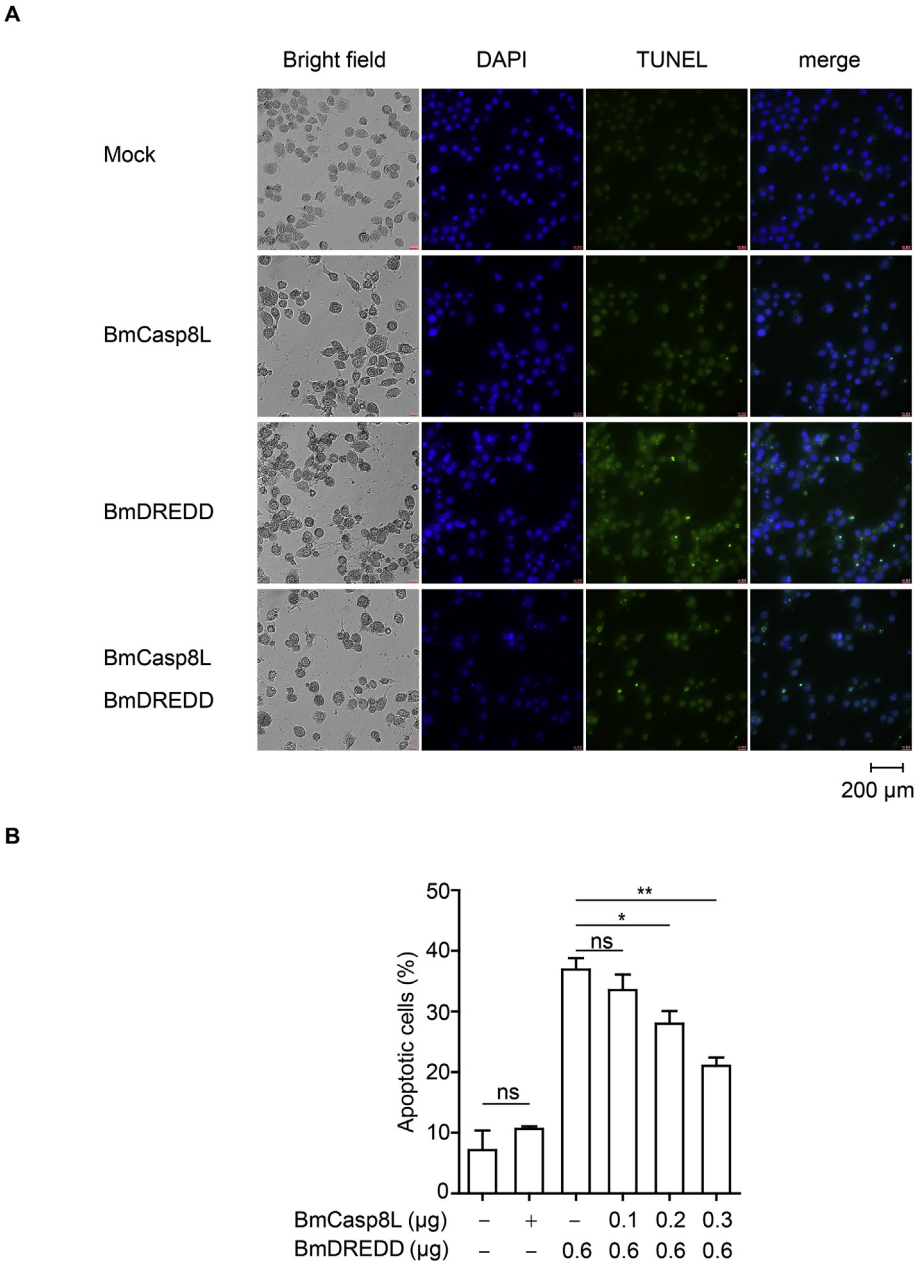

Fig. 4. BmCasp8L suppresses BmDREDD-induced apoptosis. (A) Fluorescence images of TUNEL staining of BmE cells transfected with BmDREDD alone or together with BmCasp8L. (B) Quantitative analysis of TUNEL$^+$ cells transfected with BmDREDD together with increasing amount of BmCasp8L.

Fluorescence microscopy showed that co-expression of BmCasp8L resulted in less TUNEL$^+$ cells than expression of BmDREDD alone (Fig. 4A). In addition, this reduction was dose-dependent on BmCasp8L, as apoptotic rate stepped down from 40% to 20% with increasing amount of BmCasp8L (Fig. 4B).

3.4. *BmCasp8L displays amyloidal activity*

Since tandem DED repeats have been reported to mediate the assembly of signaling complex, such as DISC and inflammasome in which caspase-8 participates (Dickens et al., 2012; Vajjhala et al., 2015), we wondered whether BmCasp8L can form similar DED filaments as caspase-8. Fluorescent microscopy revealed certain aggregates in cells transfected with construct encoding EGFP tagged-BmCasp8L (Casp8L-EGFP), although they do not look like typical fibril structures (Fig. 5A). We suspected those aggregates might be amyloid-like polymers, since two other death domain (DD) superfamily members, PYD (pyrin domain) and CARD (caspase recruitment domain) possess prion-like properties (Cai et al., 2014). We tested it by adding Thioflavin T (ThT) which binds to amyloid polymers and changes their spectral properties to BmCasp8L protein expressed and purified from *E. coli*, then measured fluorescence after excitation at 430 nm. Surprisingly, ThT fluorescence spectra displayed an emission peak around 490 nm upon binding with BmCasp8L, like Aβ protein used as positive control (Fig. 5B). In addition, when visualizing the aggregates under electron microscopy, we found they displayed filamentous morphology, consistent with the nature of amyloids (Fig. 5C). To further investigate the amyloids aggregates *in vivo*, we stained cells expressing mCherry tagged-BmCasp8L (Casp8L-mCherry) with ThT by taking advantage of its fluorescent properties. BmCasp8L showed ThT fluorescence, which overlapped with the mCherry signal (Fig. 5D). In addition, we used semi-denaturing detergent agarose gel electrophoresis (SDD-AGE), a technique that identifies detergent resistant aggregates, such as amyloid aggregates to analyze BmCasp8L. It showed that BmCasp8L formed large aggregates

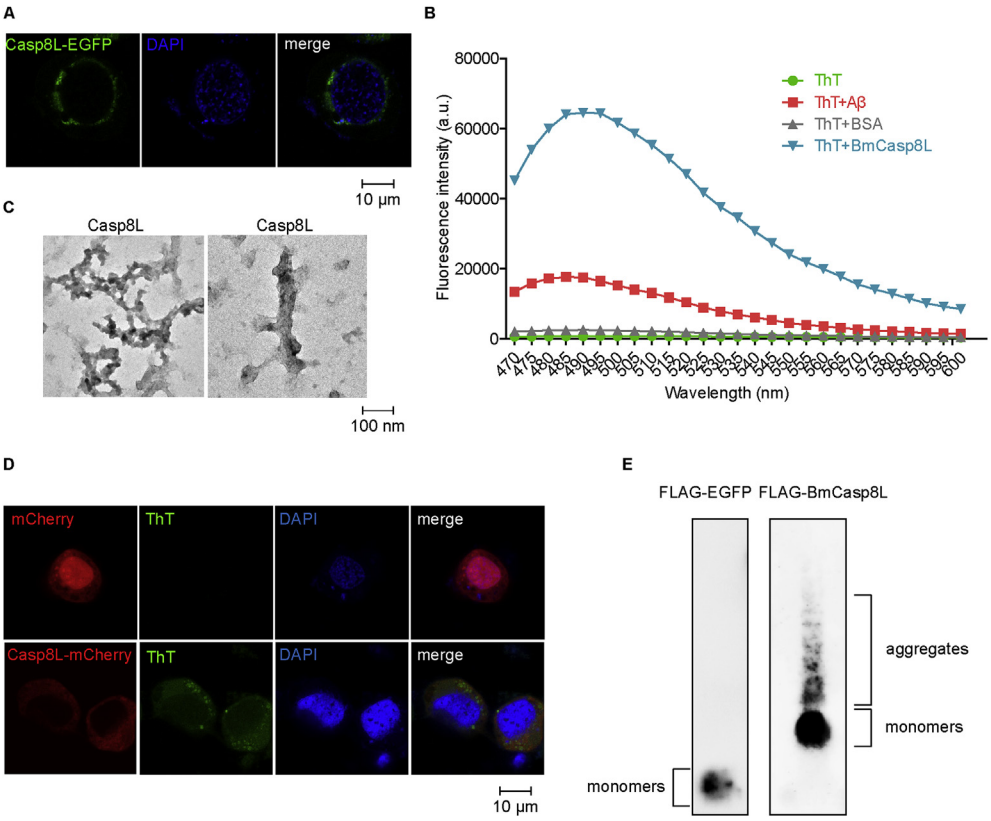

Fig. 5. BmCasp8L forms amyloidal aggregates *in vitro* and *in vivo*. (A) Immunofluorescence microscopy of cells transfected with Casp8L-EGFP. (B) ThT fluorescent emission spectra of BmCasp8L compared to Aβ and BSA. (C) Negative staining EM images of BmCasp8L. (D) BmE cells were transfected with mCherry or Casp8L-mCherry, and amyloidal aggregates were visualized by ThT fluorescence. (E) SDD-AGE profile of BmE cells lysates transfected with FLAG-BmCasp8L. FLAG-EGFP was used as negative control.

while the control EGFP was monomeric (Fig. 5E). Taken together, these results support the amyloid-like structure of BmCasp8L *in vitro* as well as *in vivo*.

3.5. *BmCasp8L is assembled with BmDREDD and BmFADD to form compact amyloid aggregates*

Since BmCasp8L attenuates the IMD signaling and apoptosis through targeting BmDREDD, which also contains tandem DEDs, we suspected they may form hetero-aggregates. ThT staining demonstrated mCherry tagged-BmDREDD (DREDD-mCherry) formed amyloid polymers alone in cells (Fig. 6A). When Casp8L-EGFP was co-expressed, the colocalization of their fluorescent signals was clearly observed (Fig. 6B). Intriguingly, a few condensed puncta appeared, which were much more prominent than in cells expressing single protein, suggesting these two proteins may be assembled into a highly-compact structure. Their direct interaction was then confirmed by co-immunoprecipitation (Fig. 6C).

We also investigated whether another DED domain-containing protein, BmFADD formed such aggregates in cells. To our surprise, it was homogeneously distributed through the cytosol (Fig. 7A), which differs with the filament structure formed by mammalian FADD (Siegel et al., 1998). Consistently, no aggregates of BmFADD were detected by SDD-AGE, while aggregates of BmDREDD were clearly visible (Fig. 7B). However, co-expression of BmDREDD dramatically changed the cellular distribution of BmFADD, they formed condensed speck-like structures similar to that were observed in cells co-expressing BmDREDD and BmCasp8L (Fig. 7A). In addition, BmCasp8L can be incorporated in the complex formed by BmDREDD and BmFADD as revealed by their overlapping fluorescence (Fig. 7C), and co-immunoprecipitation unraveled the interaction between BmCasp8L and BmFADD (Fig. 7D).

4. Discussion

In this study, we analyzed the regulatory role of a tandem DED-containing molecule, BmCasp8L. It directly suppresses BmDREDD-mediated cleavage of BmRelish and BmIMD, resulting in deficiency in PGN-induced antimicrobial peptide production. Besides its inhibitory role in the IMD pathway, it also suppresses the BmDREDD-induced apoptosis. By investigating the interaction between BmCasp8L and BmDREDD as well as BmFADD, we established that BmCasp8L forms amyloid-like aggregates as BmDREDD does, and it inactivates BmDREDD by blending into the speck-like structure formed by BmDREDD and BmFADD that is required for signaling.

Gene architecture analysis demonstrated that except in Lepidoptera, *dredd/caspase-8* in other species is encoded by multi-exon gene, which generates more than one splicing isoforms, including caspase domain-containing full length protein and caspase domain-lacking protein. Both isoforms are expressed under normal physiological conditions as discovered in *Drosophila* as well as in human, expression level of caspase domain-lacking protein is even more abundant than the full length protein, whereas their ratio may change under pathological conditions (Di Fruscio et al., 2003; Himeji et al., 2002). *Drosophila kep1* mutant has higher level of DREDD-PF and displays reduced fertility, outgrowth of extra cells and increased susceptibility to *E. coli* (Di Fruscio et al., 2003). In human, lower expression of caspase-8L was reported in peripheral blood lymphocytes from patients with systemic lupus erythematous, but higher expression in severe leukemia samples (Horiuchi et al., 2000; Mohr et al., 2005). Relations between the abnormal expression level of caspase domain-lacking protein with pathological phenotypes indicate its essential role in maintaining physiological integrity. Intron loss might have occurred to Lepidopteran *dredd* during evolution, as a result, an intronless gene emerged. Therefore, Casp8L, with the similar domain structure to the caspase domain-lacking isoforms, might substitute them for counteracting the activity of full length DREDD/caspase-8.

Activation of caspase-8 relies on the formation of DED filaments (Singh et al., 2016). DED1 of the first recruited caspase-8 molecule interacts with DED of FADD, resulting in surface exposure of the hydrophobic residues of DED2. DED2 further interacts with DED1 of

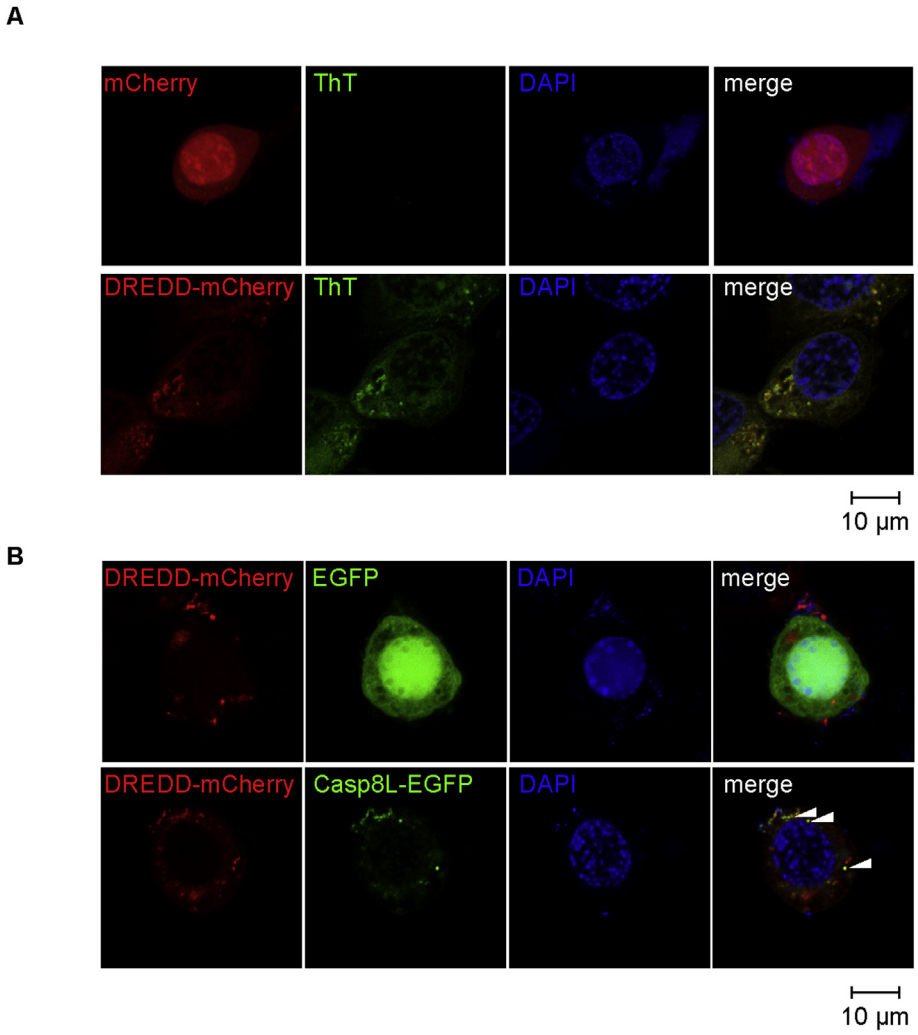

Fig. 6. BmDREDD interacts with BmCasp8L. (A) ThT fluorescence in BmE cells transfected with mCherry or DREDD-mCherry. (B) Fluorescence microscopy of cells co-transfected with DREDD-mCherry and EGFP, or with DREDD-mCherry and Casp8L-EGFP. Puncta representing colocalization of DREDD-mCherry and Casp8L-EGFP are indicated by arrowheads. (C) BmE cells were transfected with V5-BmDREDD together with FLAG-BmCasp8L or FLAG-EGFP. Cell lysates were subjected to immunoprecipitation with anti-V5 antibody. Precipitated proteins were immunoblotted with anti-FLAG antibody, and whole cell lysates as input were immunoblotted with anti-V5, anti-FLAG and anti-Tubulin antibodies.

another caspase-8 (Chen et al., 2002; Park et al., 2007). Sequential recruitment of caspase-8 results in a chain of caspase-8, which would facilitate the dimerization between neighboring caspase-8 (Dickens et al., 2012). Within the homodimer, autoproteolytic cleavage between the linker and small subunit partially activate the protein. Subsequent cleavage between DED2 and the large subunit releases the fully matured enzyme. Besides the caspase domain-missing isoform caspase-8L, another structural-related molecule, cFLIP splicing variant named cFLIPs has also been reported to inhibit caspase-8 activation (Scaffidi et al., 1999). cFLIPs is only composed of two DED repeats and incorporated into the caspase-8 filaments, leading to a decrease in the local concentration of the caspase domain of casapse-8 for dimerization and auto-processing (Krueger et al., 2001). Based on the resemblance between their characteristic tandem DEDs, we speculated BmCasp8L may exploit the similar mechanism through disrupting the alignment of neighboring DREDD (Fig. 8). Of note, the proper assembly of FADD-cappase-8 complex seems to be prerequisite for caspase-8 fully functioning, since mutation of self-processing sites in caspase-8 or *Drosophila* Dredd only affected its pro-apoptotic function but not non-apoptotic function, such as cleavage of Relish or IMD (Kang et al., 2008; Kim et al., 2014). Interaction of BmCasp8L with both BmFADD and BmDREDD may interfere with the BmFADD-BmDREDD complex,

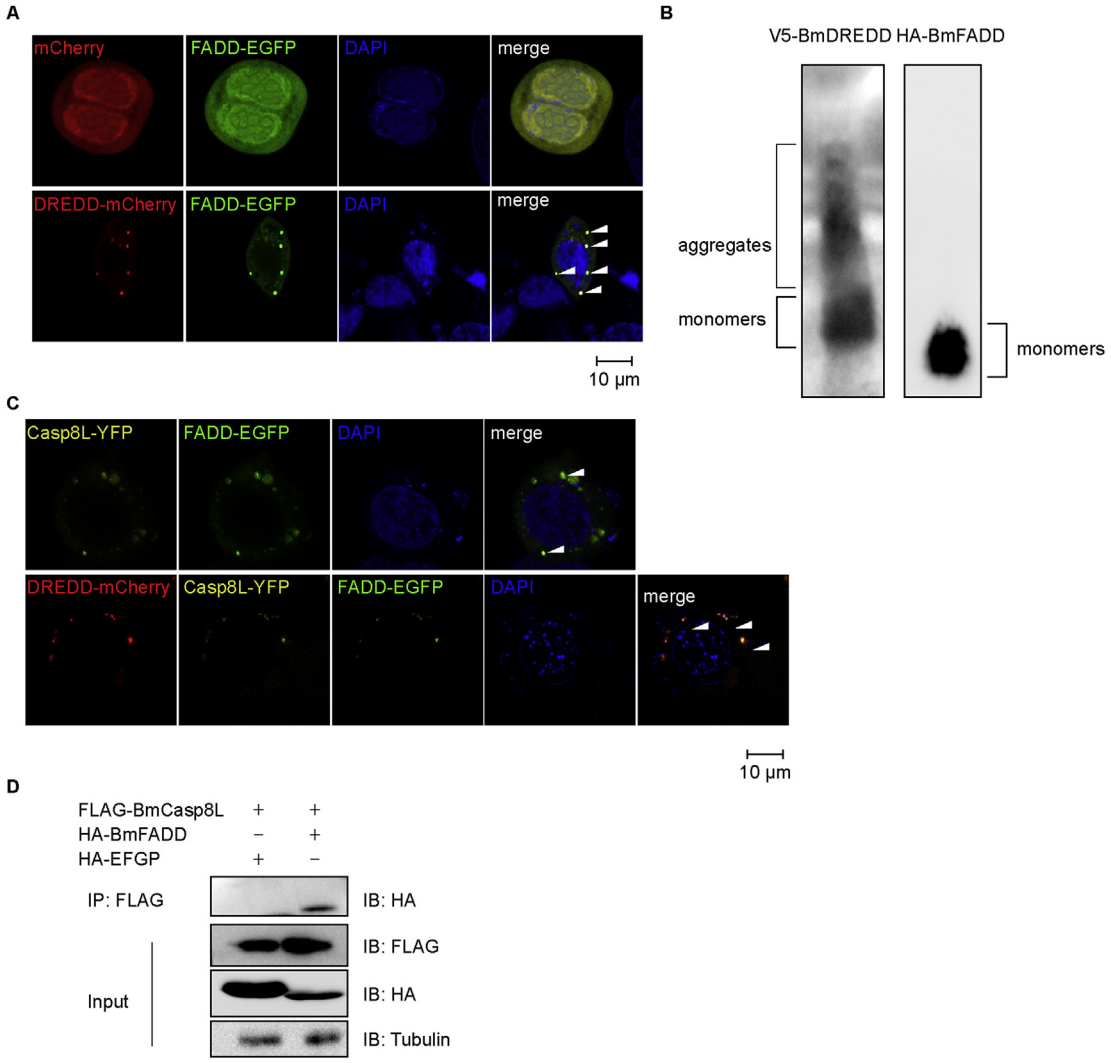

Fig. 7. BmCasp8L is assembled with BmDREDD and BmFADD to form compact amyloidal aggregates. (A) Fluorescence microscopy of cells transfected with DREDD-mCherry, FADD-EGFP, or DREDD-mCherry together with FADD-EGFP. Puncta representing colocalization of DREDD-mCherry and FADD-EGFP are indicated by arrowheads. (B) SDD-AGE profile of BmE cells lysates transfected with V5-BmDREDD or HA-BmFADD. (C) Fluorescence microscopy of cells co-transfected with Casp8L-YFP, FADD-EGFP and DREDD-mCherry. Puncta representing colocalization of Casp8L-YFP and FADD-EGFP, or colocalization of Casp8L-YFP, FADD-EGFP and DREDD-mCherry are indicated by arrowheads. (D) BmE cells were transfected with FLAG-BmCasp8L together with HA-BmFADD or HA-EGFP. Cell lysates were subjected to immunoprecipitation with anti-FLAG antibody. Precipitated proteins were immunoblotted with anti-HA antibody, and whole cell lysates as input were immunoblotted with anti-FLAG, anti-HA and anti-Tubulin antibodies.

therefore, leading to the suppression of BmDREDD.

Two upstream signaling molecules, PGRP-LC/PGRP-LE and IMD have recently been discovered to form amyloidal aggregates via their cRHIM motif (Kleino et al., 2017). The C-terminal DD of IMD is proposed to be positioned on the exterior of the amyloid fibril, which then would facilitate the interaction with FADD DD. Eventually, a supramolecular architecture could be formed after DREDD recruitment and DED chain assembly, leading to a robust signaling of IMD pathway. Similar assembly of signaling proteins via homotypic interaction between the death domains into supramolecular complexes to enable signal transduction and amplification has long been investigated in mammalian innate immunity. For instance, viral RNA sensor RIG-I (retinoic acid-inducible gene I) nucleates polymerization of MAVS (mitochondrial antiviral signaling protein) through the interaction between CARD domain on both molecules (Hou et al., 2011). Another example is ASC (apoptosis-associated speck-like protein containing a CARD), which forms prion-like fibers upon binding to cytoplasmic DNA sensor AIM2 (absent in melanoma 2) or cellular damage sensor NLRP3 (nucleotide-binding oligomerization domain, leucine rich repeat and pyrin domain containing-3) via their PYD-PYD interactions, and then through CARD-CARD interactions, the clustered ASC nucleates the formation of caspase-1 filament which allows dimerization-mediated auto-processing and activation (Proell et al., 2013). Both $MAVS^{CARD}$ and ASC^{PYD} filament exhibit prion-like properties, although they do not stain with ThT (Cai et al., 2014). Structural studies revealed that they maintain α-helical conformation within their respective fibers rather than β-sheets that are usually found in amyloids (Fu et al., 2016). However, in our study, both BmCasp8L and BmDREDD bind ThT, even they harbor DED domains that are assumed to share a common six α-helical structural fold with CARD and PYD. Whether they bear some hydrophobic cavities containing an abundance of aromatic residues that interact with or accommodate ThT, like some other non-β-sheet rich proteins such as acetylcholinesterase (Dounin et al., 2011; Sulatskaya et al., 2018), or regions connecting DED domains form β–sheet layers awaits further structural elucidation.

While BmCasp8L was initially identified as a suppressor of *Bombyx mori* STimultor of Interferon Genes (BmSTING)-mediated BmRelish activation (Hua et al., 2018), the mechanism was unknown. Since both

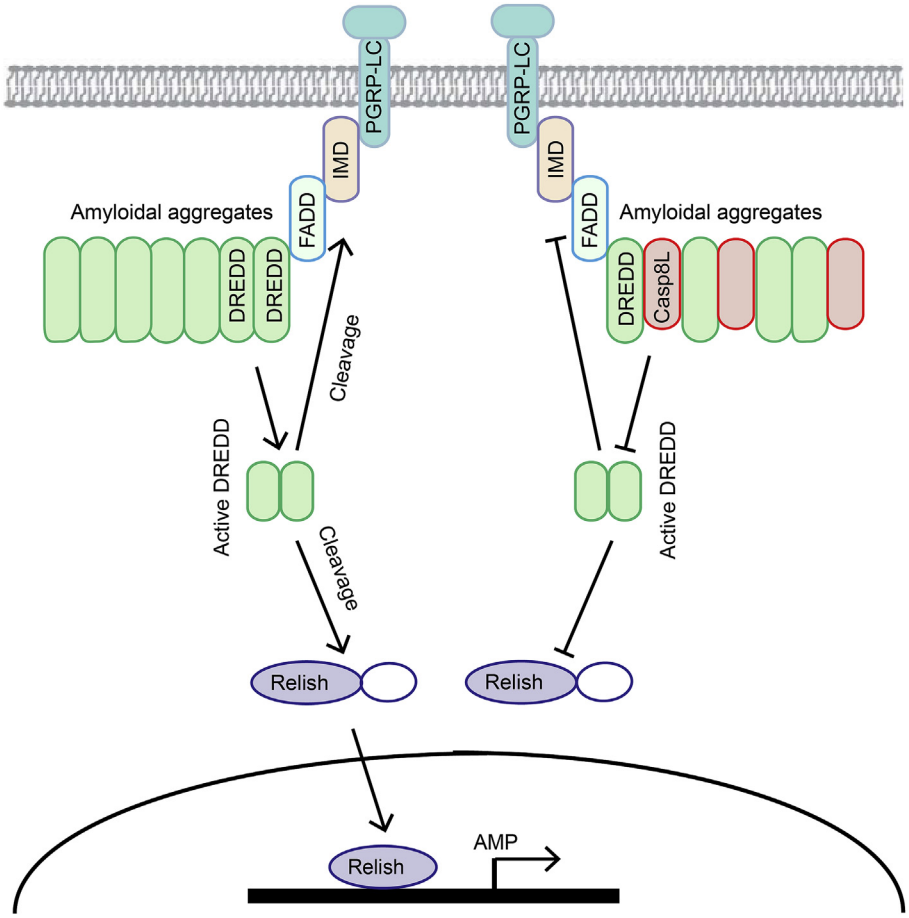

Fig. 8. A schematic diagram illustrating the mechanism of BmCasp8L for suppression of the IMD pathway. The assembly of BmFADD and BmDREDD into amyloidal aggregates facilitates the dimerization between neighboring BmDREDD. Within the homodimers, auto-cleavage occurs and activates BmDREDD, which consequently cleaves IMD and Relish. C-terminal depleted Relish is then translocated into nucleus to induce the expression of AMP. In the presence of abundant BmCasp8L, it is recruited into the amyloidal aggregates of BmFADD-BmDREDD alongside BmDREDD, leading to the heterodimer formation. As a result, BmDREDD cannot efficiently form homodimers and its activation is inhibited.

BmCasp8L and BmDREDD was co-precipitated with BmSTING, and cGAMP stimulation led to weaker interaction of BmCasp8L with BmSTING but more Relish cleavage, we suspected BmDREDD activity is subjected to the same regulation of BmCasp8L in STING pathway as it is in the IMD pathway. However, the formation of BmDREDD DED chain relies on the recruitment of BmDREDD to DED-containing protein, whether BmFADD is involved and how BmSTING participates in prompting the assembly of signaling complex needs further investigation.

To our surprise, BmFADD seems incapable of forming aggregates alone as revealed by SDD-AGE and its cellular distribution pattern, in contrast to the filament formed by the DED of human FADD (Siegel et al., 1998). The self-association of insect FADD via its own DED domain is probably too weak to form oligomer, which would explain overexpression of *Drosophila* FADD in cells did not induce apoptosis as observed in cells over-expressing human FADD (Hu and Yang, 2000). However, BmFADD is effectively incorporated into BmFADD-BmDREDD complex in a co-operative manner that is dependent on BmDREDD, as implied by the co-expression study.

It is also worth noting that the compact aggregates formed by BmFADD and BmDREDD appear similar to the ASC speck, which is considered to be a hallmark of inflammasome activation in mammalian cells (Dick et al., 2016; Hoss et al., 2017), although ASC speck can reach the size as large as 1 μm in diameter and usually appears as a single particle in most cells (Franklin et al., 2014). The downstream readout for inflammasome activation is the secretion of pro-inflammatory cytokines, such as interleukin-1β (IL-1β) and IL-18, which might be paralleled to the over-production of AMPs once Relish is activated by FADD-DREDD complex in insects. Further studies would be needed to investigate whether pyroptosis triggered by caspase-1 that is activated upon assembly of inflammasome would also be observed in insect cells.

Collectively, our results demonstrate that the tandem DED-containing protein BmCasp8L acts as a negative regulator of the IMD signaling pathway. It has amyloidal activity and interacts with both BmDREDD and BmFADD. By incorporation into the signaling complex formed by BmDREDD and BmFADD, it suppresses the activity of BmDREDD. Despite the divergence in *dredd/caspase-8* gene architecture between lepidoptera and other animals, which results in absence of caspase domain-lacking DREDD/caspase-8 splicing variants in lepidoptera as observed in other animals, the existence of BmCasp8L represents a common regulatory mechanism in innate immune signaling pathways mediated by tandem DED-containing protein.

Abbreviations

AIM2: absent in melanoma 2; AMPs: antimicrobial peptides; ASC: apoptosis-associated speck-like protein containing a CARD; CARD: caspase activation and recruitment domain; cFLIP: cellular FLICE (FADD-like IL-1β-converting enzyme)/Casp-8-like-inhibitory protein; cRHIM: cryptic RIP homotypic interaction motifs; DAP-PGN: diaminopimelic acid-type peptidoglycan; DD: death domain; DEDs: death effector domains; DREDD: Death related ced-3/Nedd2-like caspase; FADD: Fas associated via death domain; FBS: fatal bovine serun; IKK: IκB kinase; IL-1β: interleukin-1β; IMD: immune deficiency; MAVS: mitochondrial antiviral signaling protein; NLRP3: nucleotide-binding oligomerization domain, leucine rich repeat and pyrin domain containing-3; PGRP: peptidoglycan recognition protein; Pirk: poor IMD response upon knock-in; PYD: pyrin domain; qPT-PCR: quantitative reverse transcription polymerase chain reaction; PBS: Phosphate-buffered saline; RIG-I: retinoic acid-inducible gene I; RIP: receptor-interacting protein kinase; SDD-AGE: semi-denaturing detergent agarose gel electrophoresis; STING: STimultor of Interferon Genes; TAK1: transforming

growth factor (TGF)-activated kinase 1; ThT: Thioflavin T.

Funding

This work was supported by grants from the National Science Foundation of China (31530071, 31672495).

Authors' contributions

JH and FW conceived and designed the study. JH performed the experiments. XW assisted with ThT assay. XX assisted with plasmid construction. SC assisted with Western blotting. QX helped to conceive and supervised the study. JH and FW analyzed the data and wrote the manuscript. All authors read and approved the final manuscript.

Conflicts of interest

The authors declare that they have no competing interests.

Acknowledgements

We greatly appreciate Professor Yi Wang for advice in phylogenetic analysis and construction of gene architecture.

Appendix A. Supplementary data

Supplementary data to this article can be found online at https://doi.org/10.1016/j.ibmb.2019.103225.

References

Akira, S., Uematsu, S., Takeuchi, O., 2006. Pathogen recognition and innate immunity. Cell 124, 783–801.

Bonnay, F., Cohen-Berros, E., Hoffmann, M., Kim, S.Y., Boulianne, G.L., Hoffmann, J.A., Matt, N., Reichhart, J.M., 2013. *Big bang* gene modulates gut immune tolerance in *Drosophila*. Proc. Natl. Acad. Sci. U. S. A. 110, 2957–2962.

Cai, X., Chen, J., Xu, H., Liu, S., Jiang, Q.X., Halfmann, R., Chen, Z.J., 2014. Prion-like polymerization underlies signal transduction in antiviral immune defense and inflammasome activation. Cell 156, 1207–1222.

Chen, M., Orozco, A., Spencer, D.M., Wang, J., 2002. Activation of initiator caspases through a stable dimeric intermediate. J. Biol. Chem. 277, 50761–50767.

Chen, P., Rodriguez, A., Thach, T., Abrams, J.M., 1998. Dredd, a novel effector of the apoptosis activators Reaper, Grim, and Hid in *Drosophila*. Dev. Biol. 201, 202–216.

Dantoft, W., Davis, M.M., Lindvall, J.M., Tang, X., Uvell, H., Junell, A., Beskow, A., Engström, Y., 2013. The Oct1 homolog Nubbin is a repressor of NF-κB-dependent immune gene expression that increases the tolerance to gut microbiota. BMC Biol. 11, 1741–1759.

Dantoft, W., Lundin, D., Esfahani, S.S., Engström, Y., 2016. The POU/Oct transcription factor Pdm1/nub is necessary for a beneficial gut microbiota and normal lifespan of *Drosophila*. J. Innate Immun. 8, 412–426.

Di Fruscio, M., Styhler, S., Wikholm, E., Boulanger, M.C., Lasko, P., Richard, S., 2003. *Kep1* interacts genetically with *dredd/caspase-8*, and *kep1* mutants alter the balance of dredd isoforms. Proc. Natl. Acad. Sci. U. S. A. 100, 1814–1819.

Dick, M.S., Sborgi, L., Ruhl, S., Hiller, S., Broz, P., 2016. ASC filament formation serves as a signal amplification mechanism for inflammasomes. Nat. Commun. 7, 11929.

Dickens, L.S., Boyd, R.S., Jukes-Jones, R., Hughes, M.A., Robinson, G.L., Fairall, L., Schwabe, J.W., Cain, K., Macfarlane, M., 2012. A death effector domain chain DISC model reveals a crucial role for caspase-8 chain assembly in mediating apoptotic cell death. Mol. Cell 47, 291–305.

Dounin, V., Constantinof, A., Schulze, H., Bachmann, T.T., Kerman, K., 2011. Electrochemical detection of interaction between Thioflavin T and acetylcholinesterase. Analyst 136, 1234–1238.

Engel, E., Viargues, P., Mortier, M., Taillebourg, E., Couté, Y., Thevenon, D., Fauvarque, M.O., 2014. Identifying USPs regulating immune signals in *Drosophila*: USP2 deubiquitinates IMD and promotes its degradation by interacting with the proteasome. Cell Commun. Signal. 12.

Erturk-Hasdemir, D., Broemer, M., Leulier, F., Lane, W.S., Paquette, N., Hwang, D., Kim, C.H., Stöven, S., Meier, P., Silverman, N., 2009. Two roles for the *Drosophila* IKK complex in the activation of Relish and the induction of antimicrobial peptide genes. Proc. Natl. Acad. Sci. U. S. A. 106, 9779–9784.

Foley, E., O'Farrell, P.H., 2004. Functional dissection of an innate immune response by a genome-wide RNAi screen. PLoS Biol. 2, E203.

Franklin, B.S., Bossaller, L., De Nardo, D., Ratter, J.M., Stutz, A., Engels, G., Brenker, C., Nordhoff, M., Mirandola, S.R., Al-Amoudi, A., Mangan, M.S., Zimmer, S., Monks, B.G., Fricke, M., Schmidt, R.E., Espevik, T., Jones, B., Jarnicki, A.G., Hansbro, P.M., Busto, P., Marshak-Rothstein, A., Hornemann, S., Aguzzi, A., Kastenmuller, W., Latz, E., 2014. The adaptor ASC has extracellular and 'prionoid' activities that propagate inflammation. Nat. Immunol. 15, 727–737.

Fu, T.M., Li, Y., Lu, A., Li, Z., Vajjhala, P.R., Cruz, A.C., Srivastava, D.B., DiMaio, F., Penczek, P.A., Siegel, R.M., Stacey, K.J., Egelman, E.H., Wu, H., 2016. Cryo-EM structure of Caspase-8 tandem DED filament reveals assembly and regulation mechanisms of the death-inducing signaling complex. Mol. Cell 64, 236–250.

Georgel, P., Naitza, S., Kappler, C., Ferrandon, D., Zachary, D., Swimmer, C., Kopczynski, C., Duyk, G., Reichhart, J.M., Hoffmann, J.A., 2001. *Drosophila* immune deficiency (IMD) is a death domain protein that activates antibacterial defense and can promote apoptosis. Dev. Cell 1, 503–514.

Himeji, D., Horiuchi, T., Tsukamoto, H., Hayashi, K., Watanabe, T., Harada, M., 2002. Characterization of caspase-8L:a novel isoform of caspase-8 that behave as an inhibitor of the caspase. Blood 99, 4070–4078.

Horiuchi, T., Himeji, D., Tsukamoto, H., Harashima, S., Hashimura, C., Hayashi, K., 2000. Dominant expression of a novel splice variant of caspase-8 in human peripheral blood lymphocytes. Biochem. Biophys. Res. Commun. 272, 877–881.

Horn, S., Hughes, M.A., Schilling, R., Sticht, C., Tenev, T., Ploesser, M., Meier, P., Sprick, M.R., MacFarlane, M., Leverkus, M., 2017. Caspase-10 negatively regulates Caspase-8-mediated cell death, switching the response to CD95L in favor of NF-κB activation and cell survival. Cell Rep. 19, 785–797.

Hoss, F., Rodriguez-Alcazar, J.F., Latz, E., 2017. Assembly and regulation of ASC specks. Cell. Mol. Life Sci. 74, 1211–1229.

Hou, F., Sun, L., Zheng, H., Skaug, B., Jiang, Q.X., Chen, Z.J., 2011. MAVS forms functional prion-like aggregates to activate and propagate antiviral innate immune response. Cell 146, 448–461.

Hu, J., Wang, X., Wang, F., 2018. Functional characterization of BmCaspase-8-Like (BmCasp8L) as an immune negative regulatory molecule in silkworm (*Bombyx mori*). Sci. Agric. Sin. 51, 4188–4196.

Hu, S., Yang, X., 2000. dFADD, a novel death domain-containing adapter protein for the *Drosophila* caspase DREDD. J. Biol. Chem. 275, 30761–30764.

Hua, X., Li, B., Song, L., Hu, C., Li, X., Wang, D., Xiong, Y., Zhao, P., He, H., Xia, Q., Wang, F., 2018. Stimulator of interferon genes (STING) provides insect antiviral immunity by promoting Dredd caspase-mediated NF-κB activation. J. Biol. Chem. 293, 11878–11890.

Hua, X., Ma, X., Xue, R., Cheng, T., Wang, F., Xia, Q., 2016. Characterization of the *Bombyx mori* Cecropin A1 promoter regulated by IMD pathway. Insect Sci. 23, 297–304.

Kang, T.B., Oh, G.S., Scandella, E., Bolinger, B., Ludewig, B., Kovalenko, A., Wallach, D., 2008. Mutation of a self-processing site in Caspase-8 compromises its apoptotic but not its nonapoptotic functions in bacterial artificial chromosome-transgenic mice. J. Immunol. 181, 2522–2532.

Kim, C.H., Paik, D., Rus, F., Silverman, N., 2014. The caspase-8 homolog Dredd cleaves IMD and Relish but is not inhibited by p35. J. Biol. Chem. 289 20092-200101.

Kim, M., Lee, J.H., Lee, S.Y., Kim, E., Chung, J., 2006. Caspar, a suppressor of antibacterial immunity in *Drosophila*. Proc. Natl. Acad. Sci. U. S. A. 103, 16358–16363.

Kleino, A., Ramia, N.F., Bozkurt, G., Shen, Y., Nailwal, H., Huang, J., Napetschnig, J., Gangloff, M., Chan, F.K., Wu, H., Li, J., Silverman, N., 2017. Peptidoglycan-sensing receptors trigger the formation of functional amyloids of the adaptor protein IMD to initiate *Drosophila* NF-κB signaling. Immunity 47, 635–647.

Kleino, A., Silverman, N., 2014. The *Drosophila* IMD pathway in the activation of the humoral immune response. Dev. Comp. Immunol. 42, 25–35.

Kleino, A., Silverman, N., 2019. Regulation of the *Drosophila* IMD pathway by signaling amyloids. Insect Biochem. Mol. Biol. 108, 16–23.

Kleino, A., Valanne, S., Ulvila, J., Kallio, J., Myllymäki, H., Enwald, H., Stöven, S., Poidevin, M., Ueda, R., Hultmark, D., Lemaitre, B., Rämet, M., 2005. Inhibitor of apoptosis 2 and TAK1-binding protein are components of the *Drosophila* IMD pathway. EMBO J. 24, 3423–3434.

Kounatidis, I., Chtarbanova, S., Cao, Y., Hayne, M., Jayanth, D., Ganetzky, B., Ligoxygakis, P., 2017. NF-κB immunity in the brain determines fly lifespan in healthy aging and age-related neurodegeneration. Cell Rep. 19, 836–848.

Krueger, A., Schmitz, I., Baumann, S., Krammer, P.H., Kirchhoff, S., 2001. Cellular FLICE-inhibitory protein splice variants inhibit different steps of caspase-8 activation at the CD95 death-inducing signaling complex. J. Biol. Chem. 276, 20633–20640.

Libert, S., Chao, Y., Chu, X., Pletcher, S.D., 2006. Trade-offs between longevity and pathogen resistance in *Drosophila melanogaster* are mediated by NF-κB signaling. Aging Cell 5, 533–543.

Maillet, F., Bischoff, V., Vignal, C., Hoffmann, J., Royet, J., 2008. The *Drosophila* peptidoglycan recognition protein PGRP-LF blocks PGRP-LC and IMD/JNK pathway activation. Cell Host Microbe 3, 293–303.

Miller, M.A., Karacay, B., Zhu, X., O'Dorisio, M.S., Sandler, A.D., 2006. Caspase 8L, a novel inhibitory isoform of caspase 8, is associated with undifferentiated neuroblastoma. Apoptosis 11, 15–24.

Mohr, A., Zwacka, R.M., Jarmy, G., Buneker, C., Schrezenmeier, H., Dohner, K., Beltinger, C., Wiesneth, M., Debatin, K.M., Stahnke, K., 2005. Caspase-8L expression protects CD34+ hematopoietic progenitor cells and leukemic cells from CD95-mediated apoptosis. Oncogene 24, 2421–2429.

Morris, O., Liu, X., Domingues, C., Runchel, C., Chai, A., Basith, S., Tenev, T., Chen, H., Choi, S., Pennetta, G., Buchon, N., Meier, P., 2016. Signal integration by the IκB protein Pickle shapes *Drosophila* innate host defense. Cell Host Microbe 20, 283–295.

Myllymaki, H., Valanne, S., Ramet, M., 2014. The *Drosophila* IMD signaling pathway. J. Immunol. 192, 3455–3462.

Paquette, N., Broemer, M., Aggarwal, K., Chen, L., Husson, M., Erturk-Hasdemir, D., Reichhart, J.M., Meier, P., Silverman, N., 2010. Caspase-mediated cleavage, IAP binding, and ubiquitination: linking three mechanisms crucial for *Drosophila* NF-κB signaling. Mol. Cell 37, 172–182.

Park, H.H., Lo, Y.C., Lin, S.C., Wang, L., Yang, J.K., Wu, H., 2007. The death domain

superfamily in intracellular signaling of apoptosis and inflammation. Annu. Rev. Immunol. 25, 561–586.
Proell, M., Gerlic, M., Mace, P.D., Reed, J.C., Riedl, S.J., 2013. The CARD plays a critical role in ASC foci formation and inflammasome signalling. Biochem. J. 449, 613–621.
Riley, J.S., Malik, A., Holohan, C., Longley, D.B., 2015. DED or alive: assembly and regulation of the death effector domain complexes. Cell Death Dis. 6, e1866.
Royet, J., Reichhart, J.M., Hoffmann, J.A., 2005. Sensing and signaling during infection in *Drosophila*. Curr. Opin. Immunol. 17, 11–17.
Scaffidi, C., Schmitz, I., Krammer, P.H., Peter, M.E., 1999. The role of c-FLIP in modulation of CD95-induced apoptosis. J. Biol. Chem. 274, 1541–1548.
Schleich, K., Buchbinder, J.H., Pietkiewicz, S., Kahne, T., Warnken, U., Ozturk, S., Schnolzer, M., Naumann, M., Krammer, P.H., Lavrik, I.N., 2016. Molecular architecture of the DED chains at the DISC: regulation of procaspase-8 activation by short DED proteins c-FLIP and procaspase-8 prodomain. Cell Death Differ. 23, 681–694.
Siegel, R.M., Martin, D.A., Zheng, L., Ng, S.Y., Bertin, J., Cohen, J., Lenardo, M.J., 1998. Death-effector filaments: novel cytoplasmic structures that recruit caspases and trigger apoptosis. J. Cell Biol. 141, 1243–1253.
Singh, N., Hassan, A., Bose, K., 2016. Molecular basis of death effector domain chain assembly and its role in caspase-8 activation. FASEB J. 30, 186–200.
Stöven, S., Ando, I., Kadalayil, L., Engström, Y., Hultmark, D., 2000. Activation of the *Drosophila* NF-κB factor Relish by rapid endoproteolytic cleavage. EMBO Rep. 1, 347–352.
Stöven, S., Silverman, N., Junell, A., Hedengren-Olcott, M., Erturk, D., Engström, Y., Maniatis, T., Hultmark, D., 2003. Caspase-mediated processing of the *Drosophila* NF-κB factor Relish. Proc. Natl. Acad. Sci. U. S. A. 100, 5991–5996.
Sulatskaya, A.I., Rychkov, G.N., Sulatsky, M.I., Rodina, N.P., Kuznetsova, I.M., Turoverov, K.K., 2018. Thioflavin T interaction with acetylcholinesterase: new evidence of 1:1 binding stoichiometry obtained with samples prepared by equilibrium microdialysis. ACS Chem. Neurosci. 9, 1793–1801.
Vajjhala, P.R., Lu, A., Brown, D.L., Pang, S.W., Sagulenko, V., Sester, D.P., Cridland, S.O., Hill, J.M., Schroder, K., Stow, J.L., Wu, H., Stacey, K.J., 2015. The inflammasome adaptor ASC induces procaspase-8 death effector domain filaments. J. Biol. Chem. 290, 29217–29230.
Wang, L., Song, J., Bao, X.Y., Chen, P., Yi, H.S., Pan, M.H., Lu, C., 2016. BmDredd is an initiator caspase and participates in Emodin-induced apoptosis in the silkworm, *Bombyx mori*. Gene 591, 362–368.